

Ultrafast electron relaxation via breathing vibration of gold nanocrystals embedded in a dielectric medium

Y. Hamanaka and J. Kuwabata

Center for Integrated Research in Science and Engineering and Department of Crystalline Materials Science, Nagoya University, Chikusa-ku, Nagoya 464-8603, Japan

I. Tanahashi

R&D Planning Office, Matsushita Electric Industrial Co. Ltd., Moriguchi, Osaka 670-8501, Japan

S. Omi

R&D Center, HOYA Corporation, Akishima, Tokyo 196-8510, Japan

A. Nakamura

Center for Integrated Research in Science and Engineering and Department of Crystalline Materials Science, Nagoya University, Chikusa-ku, Nagoya 464-8603, Japan

and CREST, JST (Japan Science and Technology), Shibuya-ku, Tokyo 150-0002, Japan

(Received 8 June 2000; published 15 February 2001)

Relaxation dynamics of electrons in gold nanocrystals with diameters of 3.0–17.5 nm embedded in SiO₂, Al₂O₃, and TiO₂ matrices have been investigated by means of femtosecond pump and probe spectroscopy. The experiments show that the energy relaxation rates depend on both the nanocrystal size and the matrix material. A model taking account of electron-breathing mode interaction, electron-bulk phonon interaction, and thermal diffusion through the interface can explain well the observed results. The breathing mode damping in the medium on a time scale of a few picoseconds plays an important role in the electron-energy dissipation process of the nanoscale composite system.

DOI: 10.1103/PhysRevB.63.104302

PACS number(s): 78.47.+p, 63.22.+m, 73.20.Mf, 73.63.–b

The nonequilibrium dynamics of laser-heated conduction electrons in metals and semiconductors with a nanometer size in composite systems is a fascinating area of intense research because of a variety of physical properties of inclusions and environments. In metal and semiconductor nanocrystals, three-dimensional confinement effects imposed by the surrounding medium lead to pronounced modifications of electronic and optical properties.^{1–3} Lattice vibrations are also confined, generating surface modes characteristic of shape and boundary conditions at the interface.⁴

Metal nanocrystal-dielectric composites have been intensively investigated because of fast electron dynamics and high nonlinear optical susceptibilities associated with surface plasmon (SP) resonance.^{5–13} As the electron heat capacity of metal is one to two orders of magnitude smaller than the lattice heat capacity, the electron gas is easily heated to a temperature T_e up to several thousand K, while keeping the lattice temperature T_l relatively low.^{14–16} Most of the dynamical properties in the literature have been discussed on the basis of the models developed for bulk materials. Cooling dynamics of hot electrons to the lattice system has been interpreted in terms of the two-temperature model in which the electron-bulk phonon interaction plays a key role in relaxation.^{7–12} In contrast, Nisoli *et al.* have reported that in gallium nanoparticles, the particle-size-dependent relaxation is uniquely governed by the energy exchange with the surface phonons of metal particles disconnected with a surrounding.¹⁶ In general, however, the acoustic energy damping through the contact between the surrounding medium and the particle must take a part of relaxation processes

to form a new thermal equilibrium in the composite system. An effect of interplay between the metal nanocrystal and matrix on hot-electron relaxation on a subpicosecond time region is still an open question.

In this paper, we present a femtosecond time-resolved study of nonequilibrium electron dynamics in gold nanocrystals with diameters of 3.0–17.5 nm embedded in SiO₂, Al₂O₃, and TiO₂ matrices. We have observed diameter- and matrix-dependent decay behaviors of SP resonance signals and coherent acoustic mode oscillation. A model taking account of relaxation via electron-bulk phonon interaction, damping via electron-nanocrystal breathing mode interaction and thermal diffusion through the interface can explain well the observed diameter-dependence of the relaxation time. The results clearly demonstrate an important role of impulsive excitation and damping of breathing modes in relaxation of laser-heated electrons to the environment.

Gold nanocrystal-dielectric composites have been prepared by magnetron sputtering method.¹⁷ We used three matrix materials. Their thermal conductivities (bulk moduli) are 1.38 W m⁻¹ K⁻¹ (3.8×10^{10} N m⁻²) for SiO₂ glass, 36 W m⁻¹ K⁻¹ (1.7×10^{11} N m⁻²) for Al₂O₃, and 8.4 W m⁻¹ K⁻¹ (1.6×10^{11} N m⁻²) for TiO₂.^{18,19} Average diameters were determined from analysis of the x-ray diffraction patterns using the Scherrer formula. The diameters were 3.9, 4.9, 7.0, and 17.5 nm for SiO₂ glass matrix, 3.0, 4.2, and 6.0 nm for Al₂O₃ matrix, and 4.6 and 7.0 nm for TiO₂ matrix, respectively. Time evolutions of transient absorption spectrum have been measured by a pump and probe method with a 150 fs pulse from an amplified Ti:sapphire

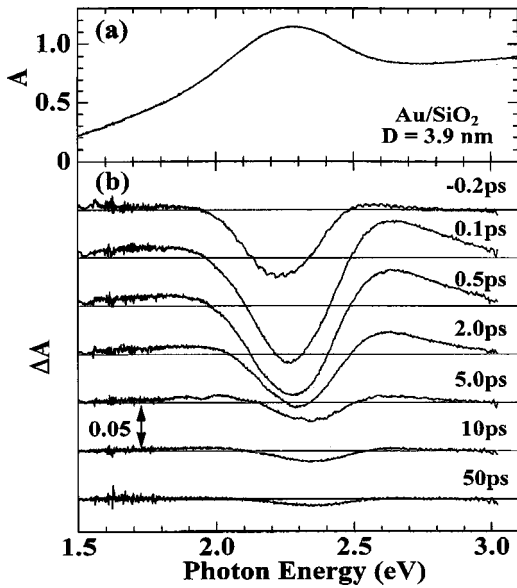


FIG. 1. (a) Absorption spectrum of Au/SiO₂ with a diameter of 3.9 nm. (b) Differential absorption spectra measured at various delay times after excitation by pump pulses.

laser. The photon energy of the pump pulse was set to about 3.1 eV corresponding to the band-to-band transition associated with $5d$ electrons of gold nanocrystals.³

Figure 1(a) shows an absorption spectrum of gold nanocrystals embedded in SiO₂ glass (Au/SiO₂) with an average diameter of 3.9 nm. The absorption peak at ~ 2.3 eV is ascribed to the SP band. The shoulder band on the high energy side of the SP peak corresponds to the band-to-band transition of gold nanocrystals.³ Differential absorption spectra were measured at various delay times between the pump and probe pulses, and the results are shown in Fig. 1(b). After the pump pulse excitation, differential absorption ΔA decreases around the peak energy of the SP band, while ΔA increases on both the high and low energy sides of the peak. As the delay time proceeds, ΔA decreases, keeping the spectral feature almost constant. Similar spectral and temporal behaviors were observed for all the samples studied here. As was observed for silver nanocrystals in glass, these spectral features are mainly ascribed to broadening the SP band due to the modification of dielectric functions induced by the creation of nonequilibrium electrons in metal nanocrystals.^{7–10,12,20,21}

To investigate electron dynamics, we measured time evolutions of ΔA at the peak photon energy of the SP resonance. A pump intensity was adjusted so that an absorbed pump energy by unit volume of nanocrystals was kept constant for the measurement. The pump energies were 3.5×10^2 and 7.0×10^2 J cm⁻³ for all the samples of Au/SiO₂ and Au/Al₂O₃, respectively. As shown in Fig. 2(a), the observed decay kinetics clearly indicate size-dependent behaviors. The relaxation times τ_1 , obtained by fitting the data to an exponential function are 2.3, 2.8, 3.3, and 5.0 ps for the diameters of 3.9, 4.9, 7.0, and 17.5 nm, respectively. The diameter-dependence of τ_1 is summarized in Fig. 3(a). The relaxation becomes fast with decreasing nanocrystal diameter. Similar behaviors were observed for Au/Al₂O₃. The obtained values

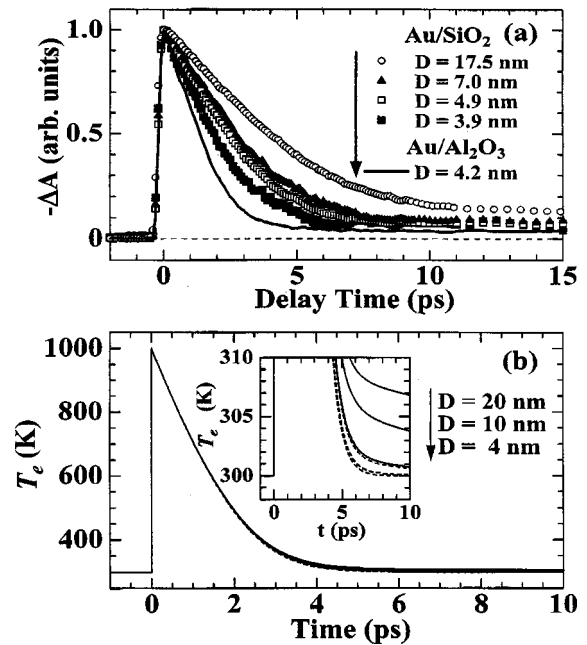


FIG. 2. (a) Time evolutions of differential absorption at the SP peak energy for Au/SiO₂ (3.9, 4.9, 7.0, and 17.5 nm) and Au/Al₂O₃ (4.2 nm). (b) Time evolutions of electron temperature T_e calculated for Au/SiO₂ (solid curves) and Au/Al₂O₃ (dashed curves). Nanocrystal diameters are 20, 10, and 4 nm from the top curve to the bottom. The inset is the time evolutions of T_e on an enlarged scale.

of τ_1 are plotted as a function of diameter in Fig. 3(b). The notable result is that τ_1 is shorter for Au/Al₂O₃ than for Au/SiO₂. As an example, we show as a solid curve in Fig. 2(a) the decay curve for Au/Al₂O₃ with a diameter of 4.2 nm. The decay is faster than for Au/SiO₂ for any diameter in the range of 3.9–17.5 nm. Consequently, these results indicate that the cooling dynamics of nonequilibrium electrons is strongly dependent on the matrix as well as the diameter, which suggest that the thermal conductivity or the bulk modulus is one of the parameters governing the relaxation processes.

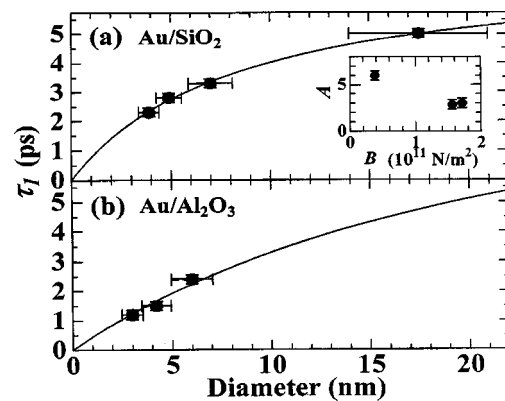


FIG. 3. Diameter dependence of relaxation times for (a) Au/SiO₂ and (b) Au/Al₂O₃. Closed circles indicate experimental results. Solid curves are fitted ones with $A = 6.0$ (a) and 3.0 (b). The inset shows a plot of the A value versus the bulk modulus B of matrices (SiO₂ glass, TiO₂, and Al₂O₃).

In line with the above argument, we analyzed quantitatively relaxation dynamics of hot electrons using the existing model. In the metal nanocrystal-dielectric composites, the energy relaxation of laser-heated electrons has been explained by the following two-step process.^{22,23} The first step is the temperature equilibrium process between electron and lattice systems via an electron-bulk phonon interaction, appearing in the time region of several ps. The second step is a thermal conduction from nanocrystals to a matrix, lasting for a few hundred ps. As the time region of the second process is two orders of magnitude longer than that of the first process, these processes have been separately analyzed in the literature.^{22,23} In this study, however, we analyze them as a parallel process taking place simultaneously. In the extended two-temperature model, time evolutions of metal-electron temperature $T_e(t)$, metal-lattice temperature $T_l(t)$, and matrix temperature $T_d(t,r)$ are given by the following coupled differential equations:

$$C_e \frac{dT_e(t)}{dt} = -G\{T_e(t) - T_l(t)\} + P(t), \quad (1)$$

$$C_l \frac{dT_l(t)}{dt} = G\{T_e(t) - T_l(t)\} - \frac{\frac{\partial}{\partial t} \left[C_d \int_R^\infty 4\pi r^2 \{T_d(t,r) - T_0\} dr \right]}{V}, \quad (2)$$

$$\frac{\partial T_d(t,r)}{\partial t} = D_d \frac{1}{r^2} \frac{\partial}{\partial r} \left[r^2 \frac{\partial T_d(t,r)}{\partial r} \right], \quad (3)$$

where C_e and C_l are the electronic and lattice specific heat capacities, respectively, and G is the electron-phonon coupling constant of metal nanocrystals. $P(t)$ is the excitation laser energy deposited by a unit volume of nanocrystals per unit time. R and V are the radius and the volume of a nanocrystal, respectively. C_d and D_d are the specific heat capacity and thermal diffusivity of the matrix, respectively, and T_0 is the initial temperature of the metal nanocrystal-dielectric composite.

Time evolutions of $T_e(t)$, $T_l(t)$, and $T_d(t,r)$ were analyzed by numerical calculations of the differential equations (1)–(3). Since the observed relaxation behaviors depend on both the size and the matrix material, it is reasonable to assume that the size dependence does not result from the electron-bulk phonon interaction in gold nanocrystals, and thus the electron-phonon coupling strength remains constant. We take the coupling constant of gold as $G = 3.0 \times 10^{16} \text{ W m}^{-3} \text{ K}^{-1}$ and use $C_e = 66 \times T_e \text{ J m}^{-3} \text{ K}^{-1}$ and $C_l = 2.49 \times 10^6 \text{ J m}^{-3} \text{ K}^{-1}$.¹⁵ C_d and D_d are $1.84 \times 10^6 \text{ J m}^{-3} \text{ K}^{-1}$ and $7.49 \times 10^{-7} \text{ m}^2 \text{ s}^{-1}$ for SiO_2 glass and $3.10 \times 10^6 \text{ J m}^{-3} \text{ K}^{-1}$ and $1.161 \times 10^{-5} \text{ m}^2 \text{ s}^{-1}$ for Al_2O_3 , respectively.¹⁸ Calculated time evolutions of $T_e(t)$ for diameters of 4, 10, and 20 nm embedded in SiO_2 glass (solid curves) and Al_2O_3 (dashed curves) are shown in Fig. 2(b). Electrons in initial equilibrium with the lattice at 300 K are heated up to 1000 K by photoexcitations with a pump

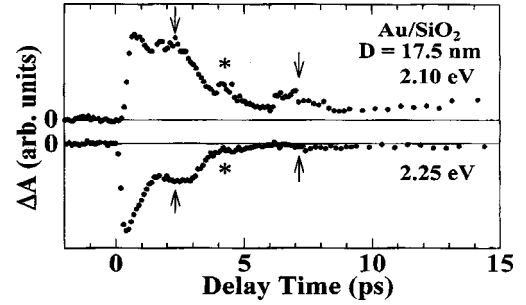


FIG. 4. Time evolutions of differential absorption for Au/SiO₂ with a diameter of 17.5 nm measured at 2.10 (upper curve) and 2.25 eV (lower curve) with the pump intensity of $0.4 \times 10^2 \text{ J cm}^{-3}$. The oscillatory structures due to the breathing mode and the second-order mode are marked by the arrows and asterisks, respectively.

intensity of $0.3 \times 10^2 \text{ J cm}^{-3}$, and then cooled down to 300 K. The calculated behaviors of $T_e(t)$ for different sizes and matrix materials are almost the same, though a small difference is noticed after 4 ps. In the inset of Fig. 2(b) illustrated with the expanded scale, we see that $T_e(t)$ decreases more rapidly for smaller nanocrystals and for Al_2O_3 in which the thermal conductivity is larger. Such behaviors do not change even when electrons are heated up to 1500 and 2000 K by photoexcitations. Therefore, it is found that the calculated dependence of $T_e(t)$ on size and matrix is much smaller than the observed dependence, and the extended two-temperature model cannot reproduce the experimental results. These results suggest that there exists another relaxation pathway giving rise to the size and matrix dependence, which is not involved in the two-step process.

Here, we consider a breathing vibration of nanocrystals that is characteristic of nanoscale particles. Excitation and damping of coherent acoustic vibrations of metal nanocrystals by the femtosecond pulses have been observed for gallium, tin, gold, and silver nanocrystals embedded in dielectrics.^{24–26} In our sample of Au/SiO₂ with a diameter of 17.5 nm, we could observe a similar oscillatory behavior on the decay curve of ΔA , when the pump intensity was decreased to $0.4 \times 10^2 \text{ J cm}^{-3}$. The oscillation is due to modulation of the SP resonance frequency by the breathing mode.²⁵ As the broadening of the SP band due to electron-electron and electron-surface collisions dominates over the spectral change in the case of the high pump intensity, the SP peak change giving rise to an oscillation behavior is obscured. Figure 4 indicates the decay curve modulated with an oscillation period of ~ 5 ps. Assuming a boundary condition of a free sphere, the period of the fundamental (breathing) mode is given by

$$T_{osc} = \frac{2\pi R}{2.93v_l}, \quad (4)$$

where v_l is the longitudinal sound velocity.²⁶ Using the value of v_l as the bulk parameter of gold crystals, T_{osc} is obtained to be 5.8 ps, which is in good agreement with our observation. The small peak seen at ~ 4.3 ps (indicated by asterisk) is ascribed to the modulation due to the second-order mode. The oscillation period due to this mode is calculated to be

2.7 ps, thus the first and second peaks are expected to appear at 1.35 and 4.05 ps, respectively. Although the first peak cannot be observed because of the large modulation due to the breathing mode, the second peak is observed at ~ 4.3 ps.

The breathing mode coherently excited by the optical pulse is damped by the damping process due to expansion of spherical waves, which was observed for silver nanocrystals.²⁵ Assuming a homogeneous elastic sphere and an infinite medium, the damping time τ_b is given by

$$\tau_b \approx \frac{AR}{v_l}, \quad (5)$$

where A is a constant defined by elastic constants of metal nanocrystals and a matrix, and a degree of the nanocrystal-matrix contact at the interface.²⁵ Mechanical vibrations of the breathing mode result in deformation potential coupling between an electron and the lattice, and modulation of the electron density via a volume change. Therefore, the damping process of the breathing mode can take a part of the energy transfer of laser-heated electrons to the surrounding medium. As the frequency of the breathing mode is as low as 2×10^{11} Hz, the lattice system can be divided into two independent subsystems: bulk phonons and breathing modes. Therefore, the total relaxation rate τ_r^{-1} is given by the following equation:

$$\frac{1}{\tau_r} = \frac{1}{\tau_b} + \frac{1}{\tau_{2-T}}, \quad (6)$$

where τ_b^{-1} and τ_{2-T}^{-1} are relaxation rates via breathing modes and bulk phonon modes, respectively.

Let us analyze the observed diameter dependence of τ_1 using Eqs. (1)–(3), (5), and (6). τ_{2-T} is given by the extended two-temperature model with the parameters for the experimental conditions used in this study. The coefficient A is taken as an adjustable parameter, because A is dependent on the degree of the matrix-nanocrystal contact as well as the elastic constants of nanocrystals and matrix. The used values of $P(t)$ in Eq. (1) are 2.3×10^{15} and 4.7×10^{15} W cm⁻³ for Au/SiO₂ and Au/Al₂O₃ in our experimental conditions, re-

spectively. We show the fitted curves in Figs. 3(a) and 3(b) by solid curves. Taking the A values as 6.0 and 3.0 for Au/SiO₂ and Au/Al₂O₃, respectively, the observed dependence of the energy relaxation time can be well reproduced. The strong dependence of the A value on the surrounding material can be explained by the difference in bulk modulus between Al₂O₃ and SiO₂. The inset in Fig. 3(a) shows the dependence of the A value on the bulk moduli of SiO₂, TiO₂, and Al₂O₃. The A value is inversely proportional to the bulk modulus. This result indicates that the relaxation time (A value) is shorter (smaller) for gold nanocrystals embedded in a matrix with a larger bulk modulus. As the elastic energy is proportional to the bulk modulus, the energy that is transferred from the nanocrystals is larger for the matrix with the large bulk modulus when the same amount of the radial displacement is given by a breathing vibration. The energy transfer via breathing vibrations is much faster than the thermal conduction governed by thermal diffusion constant, because the oscillation period is as short as ~ 5 ps.

In summary, relaxation processes of laser-heated electrons have been investigated for gold nanocrystals with diameters of 3.0–17.5 nm embedded in SiO₂ and Al₂O₃ matrices. The experimental results have shown that the relaxation times τ_1 are size and matrix dependent. The model taking into account the relaxation via electron-bulk phonon interaction, damping via electron-breathing mode interaction, and thermal diffusion through the interface has explained well the experimental results. This study allowed us to find that impulsive excitation of coherent breathing modes by femtosecond pulses leads to a rapid energy transfer of the electron system to a surrounding medium on a ps time scale. Such a process is a new class of the electron-energy dissipation process that may be seen in a variety of nano-composite systems with optical and mechanical properties.

The authors acknowledge Professor Y. Kaneda for helpful discussions on the numerical calculation. This work was supported by the Grant-in-Aid for Scientific Research from the Ministry of Education, Science, Sports, and Culture of Japan.

¹For a recent review, A.P. Alivisatos, *J. Phys. Chem.* **100**, 13 226 (1996).

²T.G. Schaaff, M.N. Shafiqullin, J.T. Khoury, I. Vezmar, R.L. Whetten, W.G. Cullen, P.N. First, C. Gutiérrez-Wing, J. Ascensio, and M.J. Jose-Yacamán, *J. Phys. Chem. B* **101**, 7885 (1997).

³U. Kreibig and M. Vollmer, *Optical Properties of Metal Clusters* (Springer-Verlag, Berlin, 1995).

⁴A. Tamura, K. Higeta, and T. Ichinokawa, *J. Phys. C* **15**, 4975 (1982).

⁵F. Hache, D. Ricard, and C. Flytzanis, *J. Opt. Soc. Am. B* **3**, 1647 (1986).

⁶R.F. Haglund, Jr., L. Yang, R.H. Magruder III, J.E. Wittig, K. Becker, and R.A. Zuhr, *Opt. Lett.* **18**, 373 (1993).

⁷T. Tokizaki, A. Nakamura, S. Kaneko, K. Uchida, S. Omi, H.

Tanji, and Y. Asahara, *Appl. Phys. Lett.* **65**, 941 (1994).

⁸J.-Y. Bigot, J.-C. Merle, O. Cregut, and A. Daunois, *Phys. Rev. Lett.* **75**, 4702 (1995).

⁹T.S. Ahmadi, S.L. Logunov, and M.A. El-Sayed, *J. Phys. Chem.* **100**, 8053 (1996).

¹⁰M. Perner, P. Bost, U. Lemmer, G. von Plessen, J. Feldmann, U. Becker, M. Mennig, M. Schmitt, and H. Schmidt, *Phys. Rev. Lett.* **78**, 2192 (1997).

¹¹J. Hodak, I. Martini, and G.V. Hartland, *J. Phys. Chem. B* **102**, 6958 (1998).

¹²N. Del Fatti, F. Vallée, C. Flytzanis, Y. Hamanaka, and A. Nakamura, *Chem. Phys.* **251**, 215 (2000).

¹³H.E. Elsayed-Ali, T.B. Norris, M.A. Pessot, and G.A. Mourou, *Phys. Rev. Lett.* **58**, 1212 (1987).

¹⁴R.W. Schoenlein, W.Z. Lin, J.G. Fujimoto, and G.L. Eesley,

- Phys. Rev. Lett. **58**, 1680 (1987).
- ¹⁵R.H.M. Groeneveld, R. Sprik, and A. Lagendijk, Phys. Rev. B **51**, 11 433 (1995).
- ¹⁶M. Nisoli, S. Stagira, S. De Silvestri, A. Stella, P. Tognini, P. Cheyssac, and R. Kofman, Phys. Rev. Lett. **78**, 3575 (1997).
- ¹⁷I. Tanahashi, M. Yoshida, Y. Manabe, and T. Tohda, Surf. Rev. Lett. **3**, 1071 (1996).
- ¹⁸Y.S. Touloukian *et al.*, *Thermophysical Properties of Matter* (Plenum Press, New York, 1970).
- ¹⁹*Physical Acoustics*, edited by W.P. Mason (Academic Press, New York, 1965).
- ²⁰Y. Hamanaka, A. Nakamura, S. Omi, N. Del Fatti, F. Vallée, and C. Flytzanis, Appl. Phys. Lett. **75**, 1712 (1999).
- ²¹T.V. Shahbazyan, I.E. Perakis, and J.-Y. Bigot, Phys. Rev. Lett. **81**, 3120 (1998).
- ²²M.J. Bloemer, J.W. Haus, and P.R. Ashley, J. Opt. Soc. Am. B **7**, 790 (1990).
- ²³J.Y. Bigot, V. Halté, J.-C. Merle, and A. Daunois, Chem. Phys. **251**, 181 (2000).
- ²⁴M. Nisoli, S. De Silvestri, A. Cavalleri, A.M. Malvezzi, A. Stella, G. Lanzani, P. Cheyssac, and R. Kofman, Phys. Rev. B **55**, R13 424 (1997).
- ²⁵N. Del Fatti, C. Voisin, F. Vallée, and C. Flytzanis, J. Chem. Phys. **110**, 11 484 (1999).
- ²⁶J. Hodak, A. Henglein, and G.V. Hartland, J. Chem. Phys. **111**, 8613 (1999).